Cytotechnology (2018) 70:225–234
https://doi.org/10.1007/s10616-017-0136-x

ORIGINAL ARTICLE

Transplantation of mesenchymal stem cells modulated Cx43 and Cx45 expression in rats with myocardial infarction

Jin-yi Li · Hong-hong Ke · Yan He · Li-na Wen · Wei-yan Xu · Zhi-fu Wu · Yan-mei Zhao · Guo-qiang Zhong

Received: 21 November 2016 / Accepted: 2 September 2017 / Published online: 19 September 2017

Abstract At present, little is known about the influence of mesenchymal stem cell (MSC) transplantation on connexin43 (Cx43) and connexin45 (Cx45) remodeling in the ischemic heart. In this study, we investigated the effect of MSC transplantation on Cx43 and Cx45 remodeling in the ischemic heart. Wistar rats were subjected to left anterior descending artery ligation to induce myocardial infarction (MI) and then randomly allocated to receive an intramyocardial injection of PBS (MI group) or 5-azacytidine-induced MSCs (MSCs group). Histological examination and western blotting were performed 4 weeks after cell transplantation. We found that the MSCs exhibited plasticity by differentiating into cardiomyocyte-like cells. Gap junction remodeling after MI was characterized by a decrease in Cx43 expression and an increase in Cx45 expression. MSC transplantation modulated the MI-induced abnormalities by up-regulating Cx43 and down-regulating Cx45 expression. MSCs exhibited plasticity by differentiating into cardiomyocyte-like cells and modulated abnormal Cx43 and Cx45 remodeling following MI.

Keywords Mesenchymal stem cells · Connexins · Myocardial infarction

Introduction

Gap junctions (GJ) are hydrophilic channels comprising two hemichannels, termed connexons, where each connexon is localized in the membrane of two adjacent cells. Each connexon consists of six integral membrane proteins called connexins (Goodenough et al. 1996). Connexons are assembled from either a single type of connexin (homomeric) or multiple types of connexins (heteromeric) (Kar et al. 2012). In the heart, three main connexins have been identified, connexin40 (Cx40), connexin43 (Cx43) and connexin45 (Cx45). The major proteins expressed in different cardiac tissues are different. Some times they can co-localize in the same junction. This offers the possibility of forming different types of connexons. In the working myocardium, Cx43 is most abundantly found, whereas Cx45 is expressed in the conduction system at low levels (Desplantez et al. 2007).

GJ channels are required for normal cardiac impulse propagation and GJ remodeling is associated with enhanced arrhythmic risk (Desplantez et al. 2007). GJ remodeling has also been shown to occur in patients with heart failure from a variety of etiologies (Kostin et al. 2003). It is unclear whether GJ remodeling in heart failure results in contractile dysfunction

Jin-yi Li and Hong-hong Ke have contributed equally to this work.

J. Li · H. Ke · Y. He · L. Wen · W. Xu · Z. Wu · Y. Zhao · G. Zhong (✉)
Department of Cardiology, The First Affiliated Hospital of Guangxi Medical University, Nanning 530021, China
e-mail: 645920840@qq.com

and/or arrhythmogenesis and, if so, the mechanisms that are involved. Cx43 is reduced in the failing heart and diminished coupling resulting from reduced Cx43 expression may contribute to a reentrant arrhythmogenic substrate (Kostin et al. 2003). However, the more modest reductions in Cx43 observed in most models of heart disease are unlikely to result in altered myocardial conduction and/or abnormal rhythm generation. Cx45, the first connexin expressed in the heart, is essential for fetal development (Alcoléa et al. 1999). Recent studies found that up-regulation of Cx45 in conjunction with down-regulation of Cx43 resulted in abnormal impulse propagation and the generation of ventricular arrhythmias in heart failure. Increased myocardial expression of Cx45 results in remodeling of intercellular coupling and greater susceptibility to ventricular arrhythmias in vivo (Betsuyaku et al. 2006).

Stem cell transplantation has emerged as a potential treatment strategy for heart failure secondary to acute or chronic ischemic heart disease (van der Bogt et al. 2008). A study showed that human mesenchymal stem cells (hMSCs) express connexins and couple to one another via Cx43 and Cx40. In addition, hMSCs formed functional GJ channels with cells transfected with Cx43, Cx40 or Cx45, and in canine ventricular cardiomyocytes (Valiunas et al. 2004). These results indicate the conditions that are fundamental for the use of MSC-based therapies for heart diseases including myocardial infarction (MI). However, little is known about the influence of MSC transplantation on Cx43 and Cx45 remodeling in the ischemic heart. In the present study, we investigated the effects of MSC transplantation on Cx43 and Cx45 remodeling in the ischemic heart.

Methods

All animals received humane care in compliance with the Guidance Suggestions for the Care and Use of Laboratory Animals by the Ministry of Science and Technology of the People's Republic of China (2006).

Preparation of allogenic bone marrow mesenchymal stem cells in vitro

Bone marrow plugs were extracted from newborn Wistar rats by flushing the bone marrow cavity with complete culture medium (L-DMEM medium containing a volume fraction of 10% fetal bovine serum, Thermofisher Scientific co.Itd, Shanghai, China). After a homogeneous cell suspension was obtained, the cells were centrifuged (1500 rpm, 15 min), resuspended in complete culture medium, plated (20×10^6 cells per 25 cm^2 culture flask), and incubated at 37 °C in a humidified atmosphere with 5% CO_2 for 2 days before the first medium change. The mesenchymal population was isolated on the basis of its ability to adhere to the culture plateau. At 70–90% confluence, the cells were trypsinized (0.25% trypsin-ethylenediaminetetraacetic acid, Sigma, St. Louis, MO, USA) and were passaged to 25 cm^2 flasks at a ratio of 1:2. Third-passage MSCs were used in all experiments. MSCs were induced using 5-azacytidine at a concentration of 10 μmol/L for 24 h. After 8 weeks, the expression of α-actin, Cx43 and troponin T was detected in the MSCs. The ultrastructure of the MSCs was detected using transmission electron microscopy.

Myocardial infarction model formation and evaluation

Thirty Wistar rats (15 males and 15 females), weighing 200–250 g, were randomly divided into two groups: the MI group and the MSCs group. An MI model was induced in all rats using previously described methods (Li et al. 2009a, b). Briefly, the rats were anesthetized with an intraperitoneal injection of 10% chloral hydrate (400 mg/kg). The trachea was orally intubated with a 14 g cannula mounted on a blunt needle with a tip and the animals were ventilated with room air at a tidal volume of 0.65 mL/100 g of body weight at a frequency of 60 breaths/min. Lead II of the electrocardiogram (ECG) was continuously monitored. Following a thoracotomy, the left anterior descending coronary artery (LAD) was ligated using a 6/0 nylon suture and then the chest cavity was closed. Successful LAD occlusion was confirmed by the elevation of the ST segment (Li et al. 2009a, b). All rats were intramuscularly injected with penicillin G (800,000 U/d) (North China Pharmaceutical Group Corporation, Shijiazhuang, China) for 3 days to prevent infection.

MSC transplantation

One week after the surgical intervention, the animals were anesthetized, the trachea was orally intubated,

and a thoracotomy was performed according to the methods described above. The rats in the MSCs group (n = 15) received a direct injection of 2×10^6/100 μl MSCs into the border and center area of infarcted myocardium, whereas the rats in the MI group (n = 15) received an injection of saline alone.

Western blot analysis

Four weeks after the transplantation, the ventricular tissues from all rats were harvested. A total of 80 mg of tissue was washed with cold PBS, and then homogenized in Tris Buffer (in mM; Tris–HCl: 10; NaCl: 150, pH: 7.4) and centrifuged at 5000×*g* for 15 min at 4 °C. The supernatants were mixed with 10% Triton X-100 and centrifuged at 10,000×*g* for 15 min for western blot analysis. The protein concentration was measured using a BCA Protein Assay Kit (Bi Yun Tian Co. Ltd., Shanghai, China). The samples were boiled for 3 min with 2% β-MerSH and then 25 μg of total protein was run on a 10% SDS polyacrylamide gel (SDS-PAGE) before the separated proteins were electrophoretically transferred to polyvinylidene fluoride (PVDF) membranes (Millipore, Billerica, MA, USA). The membranes were blocked with 5% skimmed milk in PBS containing 0.1% Tween (T-PBS) and then incubated with primary antibody at a dilution of 1:500 for 1 h at room temperature. The secondary antibody was used at a dilution of 1:500. Total Cx43 and Cx45 protein-antibody complexes were detected using chemiluminescence western blotting detection reagents (Pierce, Waltham, MA, USA), and then exposed to chemiluminescence film (Pierce) at room temperature for 5–20 s. The molecular weight was calibrated using the Low Molecular Weight Calibration Kit for SDS Electrophoresis (Millipore). Goat polyclonal Cx43 antibody (1:500 dilution, Santa Cruz, Santa Cruz, CA, USA) and goat polyclonal Cx45 antibody (1:500 dilution, Santa Cruz) were used as the primary antibodies, and anti-goat horseradish peroxidase (Santa Cruz) was used as the secondary antibody. The images were analyzed using scanning densitometer and Quantity One software (Bio-Rad, Hercules, CA, USA). The band intensity of total Cx43 and Cx45 was expressed relative to that of glyceraldehyde-3-phosphate dehydrogenase (GAPDH) and normalized to the value measured from the normal zone in the MI group.

Immunofluorescence staining and examination

Samples taken from liquid nitrogen were fixed in formalin, embedded in paraffin, and sectioned at a thickness of 4 μm. All tissue sections were blocked in PBS containing 0.1% Triton X-100 and 3% normal goat serum for 30 min. For Cx43 staining, sections were incubated in rabbit anti-Cx43 antibody (1:200, Santa Cruz) at 4 °C overnight followed by washes and an exposure to fluorescein isothiocyanate (FITC)-conjugated goat anti-rabbit antibody (1:100, Santa Cruz) for 1 h. Sections were incubated with TritonX2100 at room temperature for 10 min and then blocked in 3% bovine serum albumin. For Cx45 staining, sections were incubated in goat anti-Cx45 antibody (1:200, Santa Cruz) at 4 °C overnight followed by washes and an exposure to Texas Red (TR)-conjugated donkey anti-goat antibody (1:100, Santa Cruz) for 1 h. Sections were incubated with Triton X100 at room temperature for 10 min and then blocked in 3% bovine serum albumin. All sections of ventricle were mounted with DAPI-labeled cementing agent and examined by immunoconfocal microscopy.

Examination with transmission electron microscopy

The samples were cut into small 1 mm^3 tissue blocks and soaked in 4% polyformaldehyde-0.5% glutaraldehyde liquid before they were sliced into ultrathin sections, dehydrated with an alcohol gradient, mounted on nickel screens and embedded using LR White resin. For Cx43 staining, the sections were incubated in rabbit anti-Cx43 polyclonal antibody (1:100, Santa Cruz) at 4 °C overnight, followed by incubation in goat anti-rabbit IgG-colloidal gold. For Cx45 staining, the sections were incubated in goat anti-Cx45 polyclonal antibody (1:100, Santa Cruz) at 4 °C overnight, followed by incubation in rabbit anti-goat IgG-colloidal gold (BOSTER Biological Technology co.Itd, Wuhan, China). The samples were detected using transmission electron microscopy after double staining with uranium acetate and lead citrate.

Statistical analysis

All calculations were performed with SPSS 13.0 (SPSS Inc., Chicago, IL, USA) for Windows software. Statistical significance in the ANOVA analysis for the

study groups corresponded to a confidence level of 95%. The data are presented as the mean ± standard deviation (SD) of various measurements. Differences were considered statistically significant at $P < 0.05$.

Results

Characterization of bone marrow mesenchymal stem cells

After treatment with 10 μmol/L 5-azacytidine for 15 days, the third passaged MSCs showed a short spindle shape when reseeded in the culture dish. The arrangement of MSCs formed a bamboo-like joint after 6 weeks of induction. By 8 weeks of induction, the MSCs became homogeneous and fusiform and were arranged like a network. Some of the MSCs could pulse spontaneously at a range of 10–20 beats per min. On day 15 in all the 5-azacytidine-treated MSCs, immunocytochemistry examination clearly detected α-actin and troponin T on the stress fibers with characteristic periodic striations and Cx43 at the interface between adjacent cells. The transmission electron microscopy examination showed that the cytoplasm of the MSCs was abundantly rich in organelles such as mitochondria, the endoplasmic reticulum and the Golgi apparatus after induction. Several myofilaments and structures of primitive sarcomeres were present in the cytoplasm of the MSCs. The above results can be referred to our previous studies (Li et al. 2009a, b).

Expression and distribution of Cx43

In sections of ventricle examined by immunoconfocal microscopy, the area of Cx43 immunoreactive particles decreased and the immunopositive spots were sparse and sporadic in MI group at ischemic zone at 4 weeks (Fig. 1). Marked decreases of Cx43 area and the proportion of total cell area ocucupied by Cx43 (Cx43% cell area) were observed in confocal images. In MI group, the Cx43 area was significantly decreased ($P < 0.0001$) from 3.729 ± 0.24 μm^2 at normal zone to 1.48 ± 0.021 μm^2 at ischemic zone. The Cx43% cell area in MI group was also significantly decreased ($P < 0.0001$) from 1.391 ± 0.017% cell area at normal zone to 0.627 ± 0.011% cell area at ischemic zone. At infarct zone of MI group, the Cx43 area (0.244 ± 0.016 μm^2) and the Cx43% cell area (0.019 ± 0.001% cell area) were significantly decreased (both $P < 0.0001$) when compared to ischemic zone (Fig. 1).

Compared with MI group, Cx43 area and Cx43% cell area at ischemic zone were significantly increased in MSCs group at 4 weeks. The Cx43 area at ischemic zone was significantly higher ($P < 0.0001$) in MSCs group (2.041 ± 0.039 μm^2) compared with MI group (1.48 ± 0.021 μm^2). The Cx43% cell area at ischemic zone was also significantly higher ($P < 0.0001$) in MSCs group (1.086 ± 0.06% cell area) versus MI group (0.627 ± 0.011% cell area) (Fig. 1). There were no differences of Cx43 area and Cx43% cell area at infarct zone between MI group and MSCs group.

In the MI group, western blotting analysis showed that Cx43 total protein content at the ischemic zone was significantly lower than that at the normal zone (0.35 ± 0.05 vs. 0.68 ± 0.09; $t = 12.41$, $P < 0.0001$). At the infarcted zone, Cx43 total protein content was significantly lower than that at the ischemic zone (0.24 ± 0.02 vs. 0.35 ± 0.05; $t = 7.911$, $P < 0.0001$). Compared with the ischemic zone of the MI group, Cx43 total protein content at the ischemic zone of the MSCs group was statistically higher (0.46 ± 0.03 vs. 0.35 ± 0.05; $t = 7.306$, $P < 0.0001$). There was no difference in Cx43 total protein expression at the infarcted zone between the MSCs group and MI group (Fig. 3A).

Expression and distribution of Cx45

In sections of ventricle examined by immunoconfocal microscopy, the distribution of Cx45 signal was discrete "hot spots" of staining (Fig. 2). The amount of Cx45 immunofluorescence signal was increased in the MI group examined by confocal microscopy. Marked increases of Cx45 area and the proportion of total cell area ocucupied by Cx45 (Cx45% cell area) were observed. In MI group, the Cx45 area was significantly increased ($P = 0.0033$) from 0.109 ± 0.008 μm^2 at normal zone to 0.149 ± 0.01 μm^2 at ischemic zone. The Cx45% cell area in MI group was also significantly increased ($P < 0.0001$) from 0.039 ± 0.002% cell area at normal zone to 0.063 ± 0.004% cell area at ischemic zone. In contrary, no increase of Cx45 area and the Cx45% cell area were observed at ischemic zone compared with normal zone in MSCs group (Fig. 2).

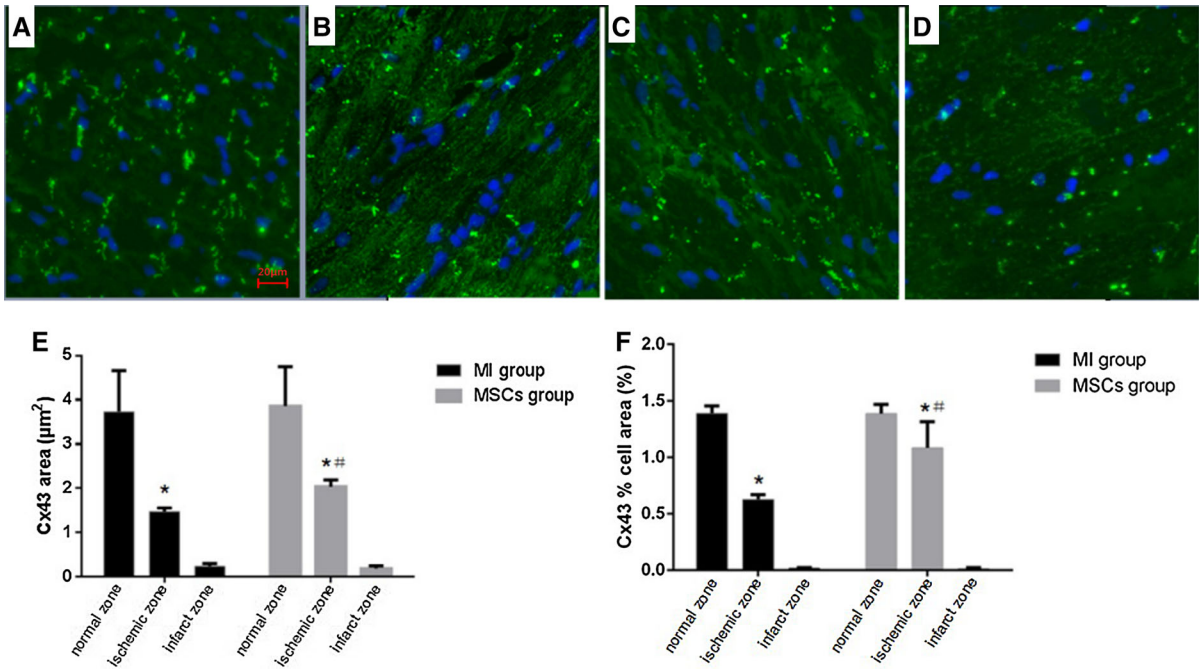

Fig. 1 Expression and distribution of Cx43 by immunofluorescence staining. **a** Confocal image of Cx43 staining by FITC (green) at normal zones showing typical gap junction staining. **b** Cx43 immunoreactive particles decreased and the immunopositive spots were sparse and sporadic at ischemic zone of MI group. **c** Cx43 immunoreactive particles at ischemic zone of MSCs group showed less degradation. **d** In infarct zone, the normal GJ structure has disappeared and Cx43 positive staining was very little. **e** Quantitative analysis showing Cx43 areas of ischemic zone both in MI group and MSCs group were significantly decreased compared with normal zone. $^{*}P < 0.0001$ versus normal zone. Cx43 area of ischemic zone in MSCs group was significantly higher than in MI group. $^{\#}P < 0.0001$ versus MI group. **f** Quantitative analysis showing Cx43% cell area of ischemic zone both in MI group and MSCs group were significantly decreased compared with normal zone. $^{*}P < 0.0001$ versus normal zone. Cx43% cell area of ischemic zone in MSCs group was significantly higher than in MI group. $^{\#}P < 0.0001$ versus MI group. (×400 magnification, scale bar = 20 μm)

Compared with the MI group, Cx45 area and Cx45% cell area at ischemic zone were significantly decreased in MSCs group at 4 weeks. The Cx45 area at ischemic zone was significantly reduced ($P = 0.0363$) in MSCs group (0.12 ± 0.009 μm^2) versus MI group (0.149 ± 0.01 μm^2). The Cx45% cell area at ischemic zone was also significantly reduced ($P = 0.0001$) in MSCs group (0.045 ± 0.002% cell area) versus MI group (0.063 ± 0.004% cell area). There was no staining of Cx45 at infarct zone both in MI group and MSCs group (Fig. 2).

In the MI group, western blotting analysis showed that Cx45 total protein expression at the ischemic zone was significantly higher than at the normal zone (0.44 ± 0.05 vs. 0.34 ± 0.08; $t = 4.105$, $P = 0.0003$). At the infarcted zone, Cx45 total protein content was significantly lower than that at the normal zone and the ischemic zone (0.12 ± 0.03 vs. 0.34 ± 0.08 and 0.44 ± 0.05, respectively; $t = 9.973$, $P < 0.0001$ and $t = 21.25$, $P < 0.0001$, respectively). Compared with the ischemic zone of the MI group, Cx45 total protein content at the ischemic zone of the MSCs group was statistically lower (0.37 ± 0.08 vs. 0.44 ± 0.05; $t = 2.874$, $P = 0.0077$). At the infarcted zone of the MSCs group, Cx45 total protein expression was significantly lower than that at the normal zone and ischemic zone (0.11 ± 0.04 vs. 0.35 ± 0.07 and 0.37 ± 0.08, respectively; $t = 11.53$, $P < 0.0001$ and $t = 11.26$, $P < 0.0001$, respectively). There was no difference in Cx45 total protein expression at the infarcted zone between the MSCs group and MI group (Fig. 3b).

Ultrastructural changes in Cx43 and Cx45

Transmission electron microscopy showed the positive expression of colloidal gold (as evidenced by black dots). In the normal area, Cx43 expression was

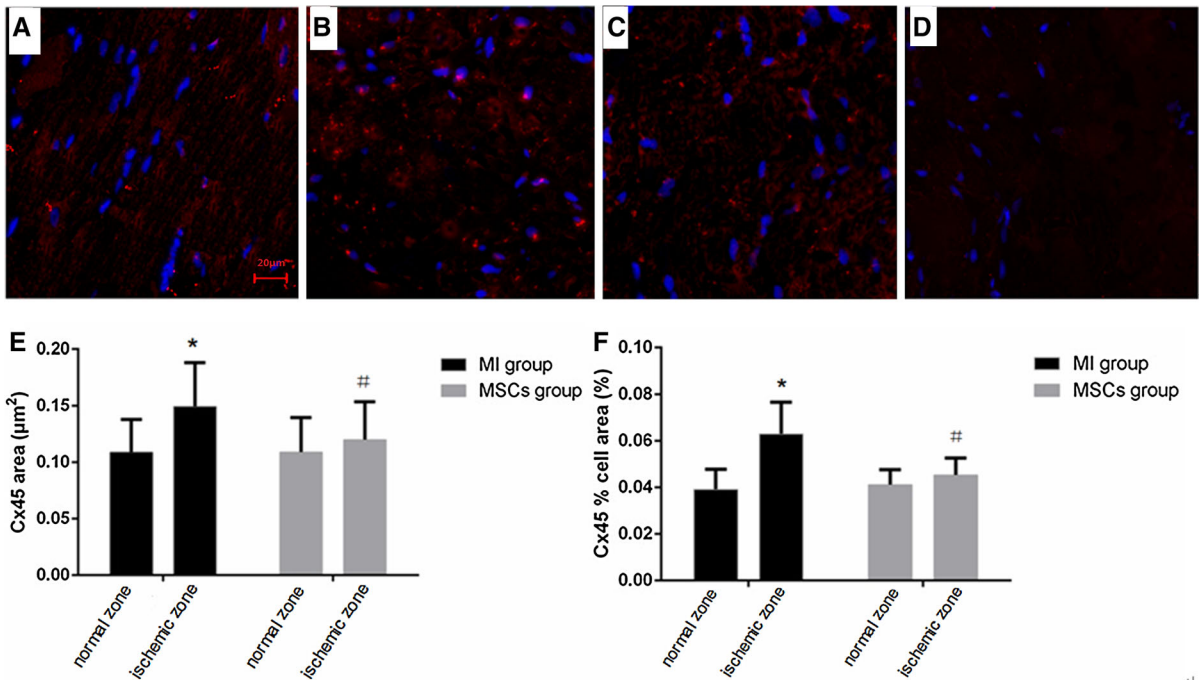

Fig. 2 Expression and distribution of Cx45 by immunofluorescence staining. **a** Confocal image of Cx45 staining by Texas Red (red) at normal zones showing the distribution of Cx45 signal as discrete "hot spots" of staining. **b** Cx45 at ischemic zone of MI group showing Cx45 immunoreactive particles were pathological increased. **c** Fluorescence stainging of Cx45 at ischemic zone of MSCs group showing less heterogeneous distribution then MI group. **d** Cx45 at infarct zone showing no of expression of staining. **e** Quantitative analysis showing Cx45 area of ischemic zone in MI group was significantly increased compared with normal zone. $^{*}P < 0.01$ versus normal zone. Cx45 area of ischemic zone in MSCs group was significantly lower than in MI group. $^{\#}P < 0.05$ versus MI group. **f** Quantitative analysis showing Cx45% cell area of ischemic zone in MI group was significantly increased compared with normal zone. $^{*}P < 0.0001$ versus normal zone. Cx45% cell area of ischemic zone in MSCs group was significantly lower than in MI group. $^{\#}P = 0.0001$ versus MI group. (×400 magnification, scale bar = 20 μm)

demonstrated as positive labeling of colloid gold. The GJ structure was clear and complete. In the MI group, the cardiomyocytes at the ischemic area were destroyed and showed a loss of normal structure. The GJ structure was ruptured with dissolution of the muscle silk. The Cx43 colloid gold labeling was sparse. In the MSCs group, Cx43 colloid gold labeling was increased in the ischemic zone and the structure of the GJ was improved. The cardiomyocytes at the infarct zone in both groups were completely necrotic and the GJs were difficult to identify. In the normal area, Cx45 colloid gold labeling was dispersed along the GJ. In the MI group, the cardiomyocytes were ruptured and hydrolyzed, with increased Cx45 colloid gold labeling at the ischemic zone. In the MSCs group, Cx45 colloid gold labeling was lower at the ischemic zone compared with the MI group, which was slightly higher than in the normal zone (Fig. 4).

Discussion

In this study, we first demonstrated that MSC transplantation, which demonstrated plasticity by differentiating into cardiomyocyte-like cells, can attenuate the abnormal myocardial Cx43 and Cx45 distribution by up-regulating Cx43 total protein expression and down-regulating Cx45 total protein expression after MI. Impairment of cell-to-cell coupling results from alterations in the expression and/or distribution (remodeling) of Cx43, which is the major constituent of cardiac GJ channels. Because Cx45 is not widely expressed in working ventricular myocytes in the normal adult heart, there are no reports on alterations of its distribution and expression during MI after MSC transplantation except for a previous study by our research group, which showed the expression of Cx43 and Cx45 mRNA following MSC transplantation in a

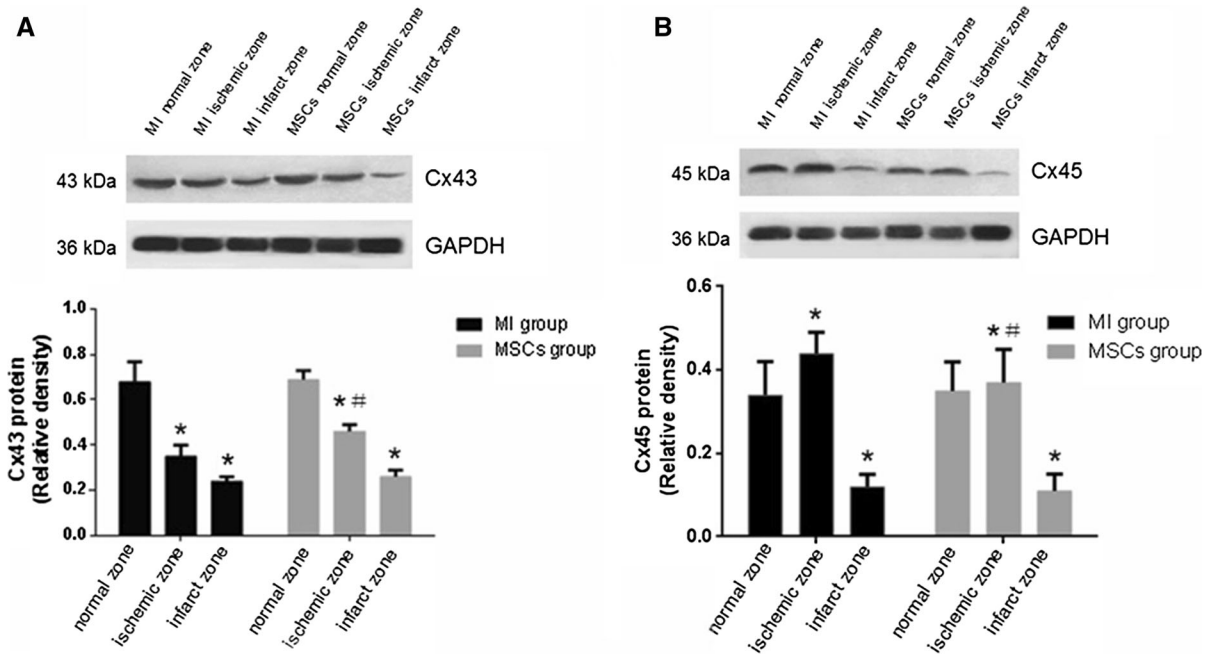

Fig. 3 Western blot analysis of Cx43 and Cx45. **a** Total Cx43 protein level at ischemic zone and infarct zone were significantly decreased compared with normal zone both in MI group and MSCs group. $^{*}P < 0.05$ versus normal zone. Total Cx43 protein level at ischemic zone in MSCs group was significantly higher than MI group. $^{\#}P < 0.05$ versus MI group. **b** Total Cx45 protein level at ischemic zone was significantly increased compared with normal zone in MI group. $^{*}P = 0.0003$ versus normal zone. Total Cx45 protein level at ischemic zone in MSCs group was significantly lower than MI group. $^{\#}P = 0.0077$ versus MI group

rat model of MI (Zhao et al. 2009). Cx43 is the major GJ protein in the adult mammalian ventricle, whereas Cx45 is expressed in special areas in the ventricle such as the conducting system. In a MI, Cx43 total protein expression is reduced and the distribution of Cx43 at the GJ is disturbed. These changes form the anatomical basis for conduction blocks, anisotropies and reentry arrhythmias. We previously reported that following MI, MSCs can modulate electrophysiological abnormalities including the PR interval, QRS duration, ventricular effective refractory period and ventricular fibrillation threshold (Li et al. 2009a, b). Here, it can be concluded that altered expression of Cx43 and Cx45 underlie, in part, the electrophysiological defects in rats with MI, which can be attenuated by reforming Cx43 and Cx45 remodeling after MSC transplantation.

The working cardiomyocytes of the ventricle are extensively interconnected by clusters of Cx43-containing GJ located at the intercalated disks (Severs et al. 2004). Two principal GJ-related alterations have been reported in the diseased ventricle: disturbances in the distribution of GJs and reduced levels of their major component, Cx43. Lateralization of Cx43 is a prominent feature of the border zone of surviving myocytes around infarct scar tissue in the human ventricle (Smith et al. 1991). By 6–12 h after ligation, the normal distribution of Cx43, desmoplakin, and cadherin was lost at the intercalated disks in the infarct zone. By 24–48 h after ligation, the expression of Cx43 was markedly decreased to 5% of the levels of sham-operated hearts (Takamatsu 2008). In a dog model of post-infarction, lateral GJ labeling in the extended infarct border zone was spatially correlated with electrophysiologically identified figure-of-eight re-entrant circuits (Peters et al. 1997). Our study showed that Cx43 protein expression was significantly reduced at the ischemic zone of MI rats after 4 weeks. Cx43 immunostaining at the ischemic zone was typically scattered in a disorderly fashion over the lateral surfaces of the cells. Fewer studies have documented alterations in the expression of Cx45 in the diseased human ventricle. Yamada et al. (2003) showed that the expression of Cx45 in the failing

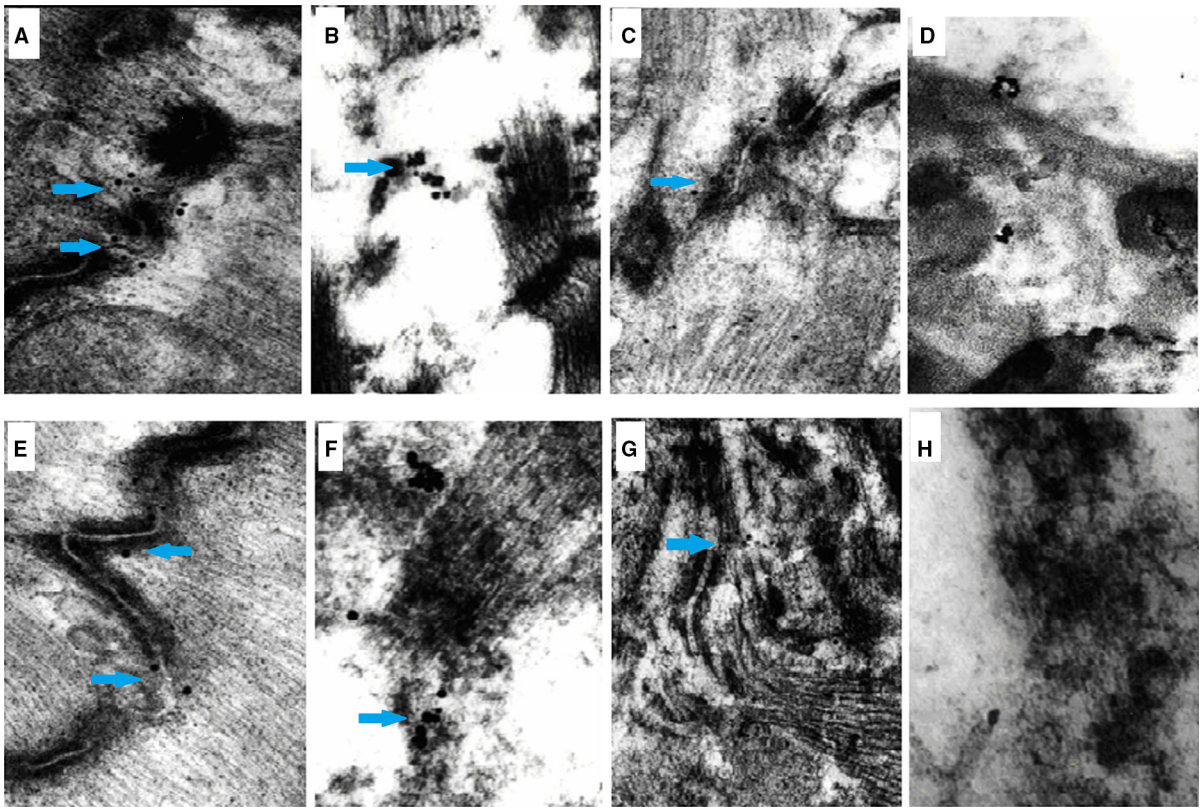

Fig. 4 Examination of Cx43 and Cx45 by transmission electric microscope. The positive expression evidenced by colloidal gold was showed as black dots (blue arrow). **a** Expression evidenced by Cx43 colloid gold in normal area. **b** Expression labeled by Cx43 colloid gold was very low at the ischemic area of MI group with the loss of normal GJ structure. **c** In MSCs group, Cx43 expression evidenced by colloid gold staining was increased in the ischemic zone. **d, h** Cardiomyocytes at the infarct zone in both groups were completely necrotic, and GJ was difficult to identify. **e** Cx45 colloid gold was dispersed along the GJ in normal area. **f** Expression of Cx45 evidenced by colloid gold at ischemic zone of MI group was increased. **g** In MSCs group, expression of Cx45 evidenced by colloid gold was lower at ischemic zone compared with MI group, which was slightly higher than that at normal zone. (×10,000 magnification)

human ventricle was up-regulated concurrently with the reduction in Cx43, which significantly altered the Cx43:Cx45 ratio. Our data showed that Cx45 mRNA was significantly increased at the ischemic zone at 4, 8 and 12 weeks in MI mice (Zhao et al. 2009).

The expression of multiple connexin isoforms induces the formation of hetero-multimeric GJ channels with distinct gating and permeability properties than their homo-multimeric counterparts. Cx43 and Cx45 can form heterotypic channels that have unitary conductances lower than those of homotypic Cx43 channels and that fail to pass the fluorescent dye Lucifer yellow (Zhong and Moreno 2002). Cx43 and Cx45 formed heteromeric channels that exhibited reduced single channel conductance compared with Cx43 homomeric channels (Martinez et al. 2002). Our data suggested that increased Cx45 expression combined with decreased Cx43 expression increased the possibility of electrophysiological abnormalities in the ischemic heart. In the absence of technology to confirm electrophysiologically that hybrid GJ channels connect ventricular myocytes in vivo, we can only speculate on the functional effects of increased Cx45 expression in the MI heart.

Stem cell transplantation has emerged as a potential treatment strategy for heart failure secondary to acute or chronic ischemic heart disease (Murry et al. 2005). 5-Azacytidine (5-Aza) induces differentiation of MSCs into cardiomyocytes. However, the underlying mechanisms are not well understood. Several studies showed that after exposure to 5-Aza, MSCs could differentiate into cardiomyocytes (Fukuda 2003).

MSCs had cardiomyocyte phenotypes after 5-Aza treatment. In addition, myogenic cells differentiated from MSCs were positive for mRNA and protein of desmin, β-myosin heavy chain, cardiac troponin T, A-type natriuretic peptide, and Nkx2.5. Sustained activation of ERK by 5-Aza contributed to the induction of the differentiation of MSCs into cardiomyocytes in vitro (Qian et al. 2012). HMSCs express connexins and couple to one another via Cx43 and Cx40. In addition, hMSCs formed functional GJ channels with cells transfected with Cx43, Cx40 or Cx45, and in canine ventricular cardiomyocytes (Valiunas et al. 2004). These results indicate the conditions that are fundamental for the use of MSC-based therapies for heart diseases including MI. Besides, cardiomyocyte transplantation has the potential to impart electrical stability to the injured heart, thereby markedly reducing the major factor leading to sudden death. This protective effect was independent of the documented modest augmentation of left ventricular function and was associated with improved electrical coupling within the infarct by the engraftment of Cx43-expressing embryonic cardiomyocytes. This enhanced coupling reduced vulnerability to ventricular tachycardia (VT) by decreasing the incidence of conduction block within the infarct and/or through a modulatory effect on the border-zone cardiomyocytes. The expression of the cardiac GJ protein Cx43 was the critical factor underlying the augmented intercellular electrical conduction and protection from arrhythmias (Roell et al. 2007). Our study demonstrated that MSC transplantation could attenuate abnormal myocardial Cx43 and Cx45 distribution, up-regulate Cx43 total protein expression and down-regulate Cx45 total protein expression after MI.

In conclusion, the left ventricular myocardium from the ischemic heart exhibited a down-regulation of Cx43 expression and an up-regulation of Cx45 expression. MSC transplantation, which could survive at the host ischemic zone and express Cx43, modulated the MI-induced electrophysiological abnormalities by up-regulating Cx43 and down-regulating Cx45.

Acknowledgements We would like to thank Drs. Ying-lin Wu and Jing-bo Jiang for their manuscript edits and revisions.

Funding This study was supported by the National Natural Science Foundation of China (No. 30560051).

Compliance with ethical standards

Conflict of interest None.

References

Alcoléa S, Théveniau-Ruissy M, Jarry-Guichard T, Marics I, Tzouanacou E, Chauvin JP, Briand JP, Moorman AF, Lamers WH, Gros DB (1999) Downregulation of connexin 45 gene products during mouse heart development. Circ Res 84:1365–1379

Betsuyaku T, Nnebe NS, Sundset R, Patibandla S, Krueger CM, Yamada KA (2006) Overexpression of cardiac connexin45 increases susceptibility to ventricular tachyarrhythmias in vivo. Am J Physiol Heart Circ Physiol 290:H163–H171

Desplantez T, Dupont E, Severs NJ, Weingart R (2007) Gap junction channels and cardiac impulse propagation. J Membr Biol 218:13–28

Fukuda K (2003) Regeneration of cardiomyocytes from bone marrow: use of mesenchymal stem cell for cardiovascular tissue engineering. Cytotechnology 41:165–175

Goodenough DA, Goliger JA, Paul DL (1996) Connexins, connexons, and intercellular communication. Annu Rev Biochem 65:475–502

Kar R, Batra N, Riquelme MA, Jiang JX (2012) Biological role of connexin intercellular channels and hemichannels. Arch Biochem Biophys 524:2–15

Kostin S, Rieger M, Dammer S, Hein S, Richter M, Klövekorn WP, Bauer EP, Schaper J (2003) Gap junction remodeling and altered connexin43 expression in the failing human heart. Mol Cell Biochem 242:135–144

Li J-Y, He Y, Wen L, Ke HH, Wei Z, Deng Y, Wu ZF (2009a) Effects of allogenic bone marrow mesenchymal stem cell transplantation on electrophysiological abnormality and left ventricular remodeling in rats with myocardial infarction. J Clin Rehabil Tissue Eng Res 13:5211–5216

Li J-Y, Zong GQ, Wei Z, Xu WY, Ke HH, Ning Z, Wu ZF (2009b) Establishment of a rat model of myocardial infarction and the post-infarction changes in electrophysiology and left ventricular function. Acta Lab Anim Sci Sin 17:419–423

Martinez AD, Hayrapetyan V, Moreno AP, Beyer EC (2002) Connexin 43 and connexin 45 form heteromeric gap junction channels in which individual components determine permeability and regulation. Circ Res 90:1100–1107

Murry CE, Field LJ, Menasché P (2005) Cell-based cardiac repair: reflections at the 10-year point. Circulation 112:3174–3183

Peters NS, Coromilas J, Severs NJ, Wit AL (1997) Disturbed connexin43 gap junction distribution correlates with the location of reentrant circuits in the epicardial border zone of healing canine infarcts that cause ventricular tachycardia. Circulation 95:988–996

Qian Q, Qian H, Zhang X, Zhu W, Yan Y, Ye S, Peng X, Li W, Xu Z, Sun L, Xu W (2012) 5-Azacytidine induces cardiac differentiation of human umbilical cord-derived mesenchymal stem cells by activating extracellular regulated kinase. Stem Cells Dev 21:67–75

Roell W, Lewalter T, Sasse P, Tallini YN, Choi BR, Breitbach M, Doran R, Becher UM, Hwang SM, Bostani T, von Maltzahn J, Hofmann A, Reining S, Eiberger B, Gabris B, Pfeifer A, Welz A, Willecke K, Salama G, Schrickel JW, Kotlikoff MI, Fleischmann BK (2007) Engraftment of connexin 43-expressing cells prevents post-infarct arrhythmia. Nature 450:819–824

Severs NJ, Coppen SR, Dupont E, Yeh HI, Ko YS, Matsushita T (2004) Gap junction alterations in human cardiac disease. Cardiovasc Res 62:368–377

Smith JH, Green CR, Peters NS, Rothery S, Severs NJ (1991) Altered patterns of gap junction distribution in ischemic heart disease. An immunohistochemical study of human myocardium using laser scanning confocal microscopy. Am J Pathol 139:801–821

Takamatsu T (2008) Arrhythmogenic substrates in myocardial infarct. Pathol Int 58:533–543

Valiunas V, Doronin S, Valiuniene L, Potapova I, Zuckerman J, Walcott B, Robinson RB, Rosen MR, Brink PR, Cohen IS (2004) Human mesenchymal stem cells make cardiac connexins and form functional gap junctions. J Physiol 555:617–626

van der Bogt KE, Sheikh AY, Schrepfer S, Hoyt G, Cao F, Ransohoff KJ, Swijnenburg RJ, Pearl J, Lee A, Fischbein M, Contag CH, Robbins RC, Wu JC (2008) Comparison of different adult stem cell types for treatment of myocardial ischemia. Circulation 118:S121–S129

Yamada KA, Rogers JG, Sundset R, Steinberg TH, Saffitz J (2003) Up-regulation of connexin45 in heart failure. J Cardiovasc Electrophysiol 14:1205–1212

Zhao YM, Li JY, He Y, Ke HH, Wang DX (2009) mRNA expression of connectin 43 and connectin 45 following transplantation of allogenic bone marrow mesenchymal stem cells in rats with acute myocardial infarction. J Clin Rehab Tissue Eng Res 13:8895–8900

Zhong G, Moreno AP (2002) The formation of mono-heteromeric Cx43-Cx45/43 gap junctions uncovers gating and selectivity properties of their channels. Biophys J 82:633b